Structure of ^{116}Sb nucleus

Z. Gácsi, Zs. Dombrádi, and T. Fényes
Institute of Nuclear Research of the Hungarian Academy of Sciences, H-4001 Debrecen, Hungary

S. Brant and V. Paar
Prirodoslovno-Matematički Fakultet, University of Zagreb, 41000 Zagreb, Croatia, Yugoslavia
(Received 23 October 1990)

The γ-ray and internal conversion electron spectra of the ^{113}In$(\alpha,n\gamma)^{116}$Sb reaction have been measured at 14.5 and 16.0 MeV bombarding α-particle energies with Ge(HP) γ and superconducting magnetic lens plus Si(Li) electron spectrometers. The energies and relative intensities of 189 ^{116}Sb γ rays (including 117 new ones), as well as internal conversion coefficients of 59 ^{116}Sb transitions, have been determined. $\gamma\gamma$ coincidences have also been measured at $E_\alpha=16$ MeV. Both low-spin and high-spin level schemes have been deduced and 32 new levels have been identified. Multipolarities of transitions and γ-ray branching ratios have been determined. The energy spectrum and electromagnetic properties have been calculated in the interacting-boson-fermion-fermion model (IBFFM), and satisfactory agreement between the experimental and theoretical results has been obtained.

I. INTRODUCTION

The level scheme of ^{116}Sb was previously studied by several groups [1–12]. Nevertheless, the spins and parities of many low-lying levels were missing or ambiguous. The ^{116}Sb level structure was not investigated earlier from $(\alpha,n\gamma)$ reaction.

The aims of the present work are a detailed γ and electron spectroscopic study of the ^{113}In$(\alpha,n\gamma)^{116}$Sb reaction, a deduction of a more complete level scheme, and an interpretation of the nuclear structure of ^{116}Sb by the interacting-boson-fermion-fermion model (IBFFM) calculation.

II. EXPERIMENTAL TECHNIQUES

For the γ- and e^--spectroscopic measurements we used 1.5–3.0- and ~ 0.5-mg/cm^2-thick self-supporting targets, respectively, which were prepared by an evaporation technique from isotopically enriched (to 93.1%) ^{113}In. For the sake of reliable γ-ray identification we have also studied the ^{115}In$+\alpha$ reaction; in these experiments an enriched (to 99.99%) ^{115}In target was used.

The targets were bombarded with $I_\alpha=1$–200 nA intensity α-beams of the Debrecen cyclotron at $E_\alpha=14.5$ and 16 MeV energies, which are several MeV higher than the corresponding (α,n) reaction Q values. The energies of γ rays were measured with a 20% Ge(HP) detector at 90° angle with respect to the beam direction. For the γ-ray intensity measurements the detector was placed at 125° angle. The energy resolution of the detector was ~ 2 keV at 1332 keV. The spectrometer was calibrated with ^{133}Ba and ^{152}Eu sources. The energies of the strong 135.52(3), 407.351(20), 542.872(20), 931.80(5), 1293.54(4) keV ^{116}Sn [7] internal calibration lines were reproduced within experimental errors.

Internal conversion electron spectra were measured with a superconducting magnetic lens spectrometer (SMLS) with Si(Li) detectors [13], in a similar way as in the case of the $(p,n\gamma)$ reaction [14]. In the $(\alpha,n\gamma)$ studies, the theoretical internal conversion coefficient (ICC) of the 307.8-keV $E2$ ^{116}Sb transition was used for normalization, because the K/L ratio of this transition indicated $E2$ multipolarity. With this normalization, all the ICC values determined in (p,n) reaction [and seen also in the (α,n) reaction] were reproduced within experimental uncertainties.

The $\gamma\gamma$-coincidence data were acquired in a two-dimensional mode at 16-MeV bombarding α-particle energy, with a fixed $\tau=50$ ns resolving time. The 20% and 25% Ge(HP) detectors were placed at 125° and 235° angles to the beam direction. [The efficiency values are relative to that of a 7.5 cm$\times$7.5 cm NaI(Tl) detector.] Approximately 56 million $\gamma\gamma$-coincidence events were recorded on magnetic tapes in event-by-event mode for subsequent analysis. After creating the symmetrized, two-parameter coincidence matrices a standard gating procedure was used. In the case of close-lying peaks a novel method was applied, using the computer code LINGAT [15], which enabled us to obtain spectra without "leak-through" in the window.

All measurements were performed with CAMAC units connected to a TPA 11/440 computer. In the data reduction we have used a γ-spectrum analysis program [16].

III. EXPERIMENTAL RESULTS

Typical γ-ray and internal conversion electron spectra are shown in Fig. 1. The internal conversion coefficients of ^{116}Sb transitions and typical $\gamma\gamma$-coincidence spectra are shown in Figs. 2 and 3, respectively.

The energies and relative intensities of γ rays assigned to ^{116}Sb, the ICC's and multipolarities of transitions, as well as the $\gamma\gamma$-coincidence relations, are given in Table I.

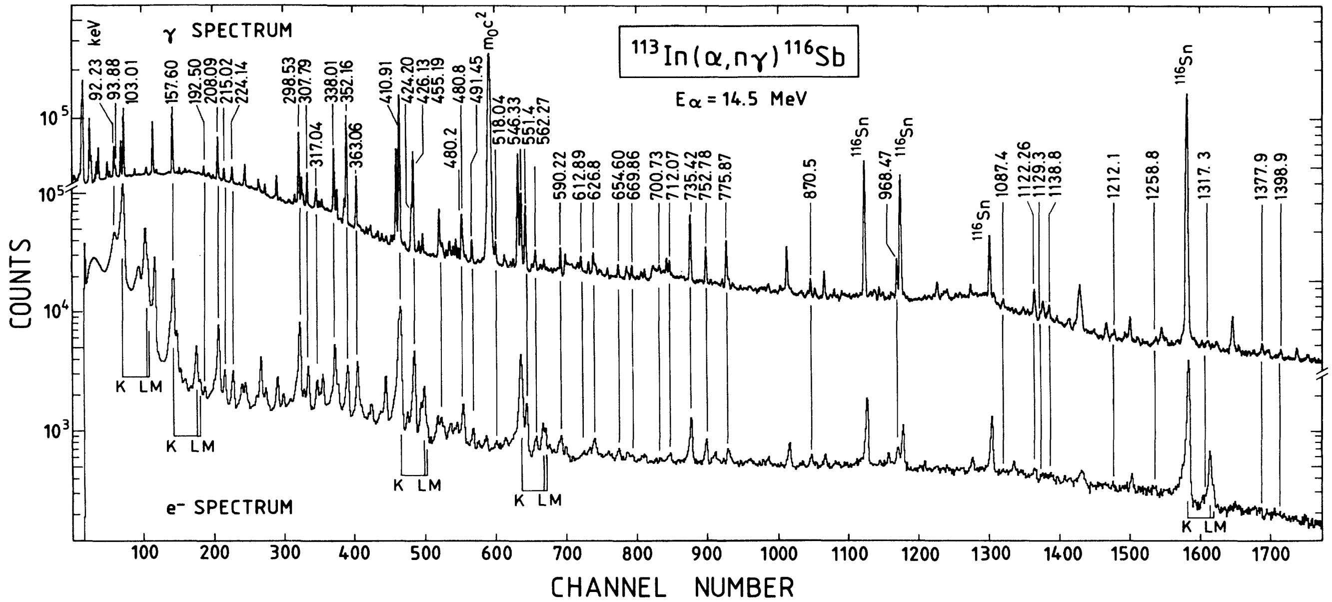

FIG. 1. Typical γ-ray and internal conversion electron spectra of the ^{113}In$(\alpha,n\gamma)^{116}$Sb reaction. The energies of γ rays are given only at the strongest ^{116}Sb lines. Corresponding conversion electron lines are also indicated.

IV. LEVEL SCHEME OF ^{116}Sb

The level schemes (Figs. 4 and 5) obtained from $(\alpha,n\gamma)$ reaction were constructed mainly on the basis of our $\gamma\gamma$-coincidence results, but the energy and intensity balance of transitions was also taken into account.

The level spin and parity assignments are based on the measured internal conversion coefficients of transitions as well as on $(p,n\gamma)$ results [14].

The low-spin level spectra obtained from $(p,n\gamma)$ (Fig. 4. of Ref. 14) and $(\alpha,n\gamma)$ reactions (Fig. 4) are similar; there are 33 levels which were observed in both reactions. On the other hand, the 731.71-keV 1^+, 1127.4-keV 2^+, 1158.48-keV 1^+, 1425.5-keV (1-3), 1481.1-keV (1-4)

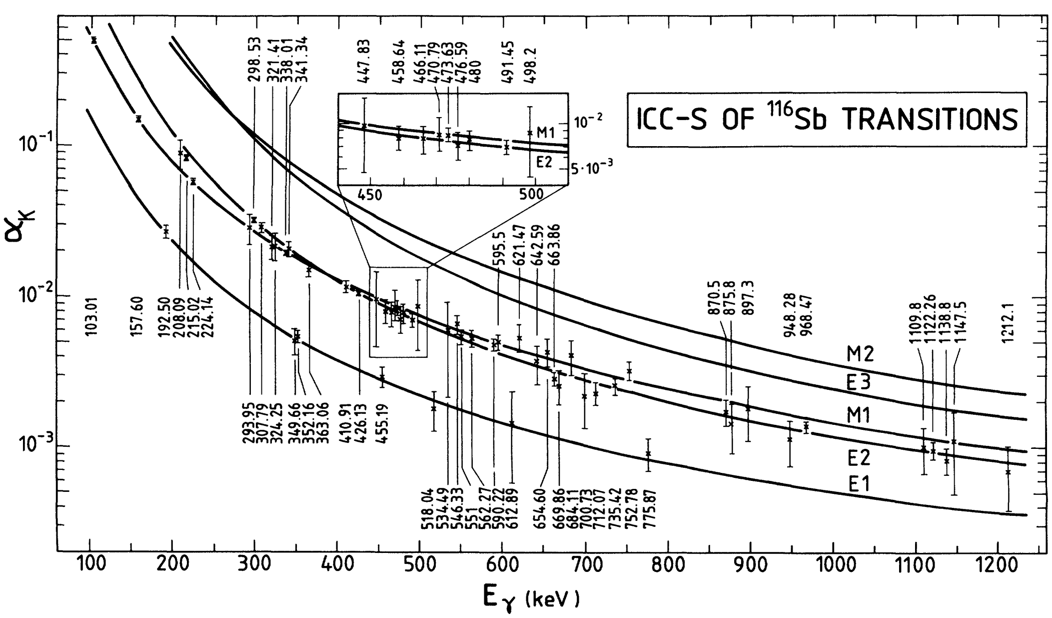

FIG. 2. Experimental internal conversion coefficients of ^{116}Sb transitions (symbols with error bars) as a function of γ-ray energy (E_γ). The curves show theoretical results [17].

states were not excited in the $(\alpha,n\gamma)$ reaction, and the 1037.68-keV $(4^+,5^+)$, 1122.26-keV 1^+-5^+, 1200.00-keV, 1208.10-keV $(4^-$-$5^-)$, 1212.04-keV $(4,3)^+$, 1312.36-keV, 1386.76-keV $(5,6)^+$, 1436.2-keV states were seen only in the $(\alpha,n\gamma)$ reaction. Owing to the higher angular momentum transfer in the latter reaction, additional high-spin ($\gtrsim 6$) states also appeared (Fig. 5). All of them decay directly (or through other high-spin states) to the 8^-, 60.3-min isomeric state. The energy of this state is not well established (Van Nes *et al.* [5] give 490±56 keV, Blachot and Marguier [7] give 383±40 keV). No γ-spectroscopic evidence was found up to now that would enable a contradiction-free connection between the low- and high-spin parts of the level scheme.

V. IBFFM/OTQM DESCRIPTION OF THE ^{116}Sb NUCLEUS

In order to get a deeper insight into the structure of the low-lying states of ^{116}Sb, we have calculated the energies and electromagnetic properties of the states on the basis of the interacting-boson-fermion-fermion/truncated-quadrupole-phonon model for odd-odd nuclei (OTQM) [18].

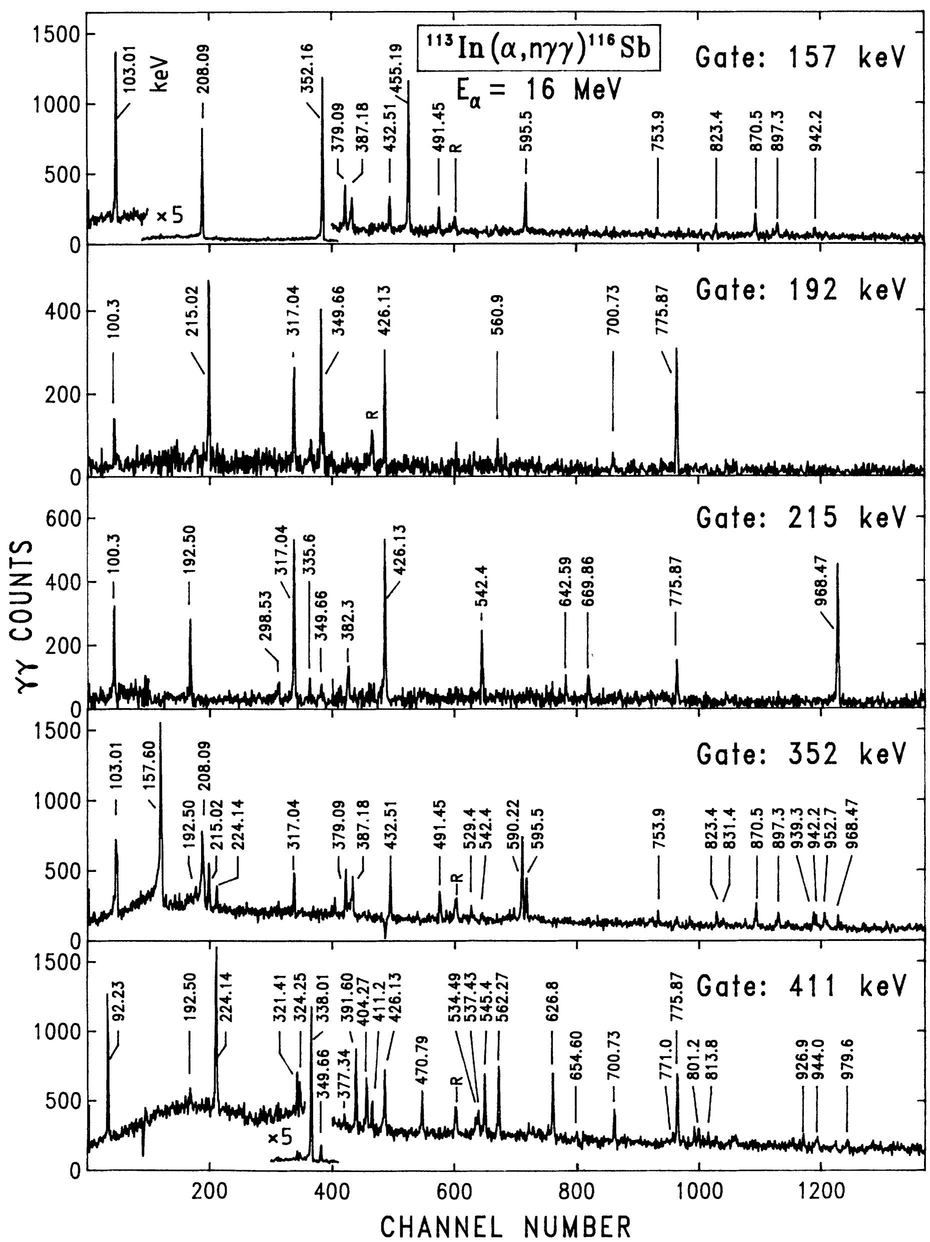

FIG. 3. Typical $\gamma\gamma$-coincidence spectra. The background was subtracted. *R* denotes random coincidences.

TABLE I. The energy ($E_{\hat{\gamma}}$) and relative intensity ($I_{\hat{\gamma}}$) of γ rays observed in ^{113}In$(\alpha,n\gamma)^{116}$Sb reaction at $E\hat{\alpha}=14.5$ MeV. Coincident γ rays were detected at $E\hat{\alpha}=16.0$ MeV. N denotes a new γ ray; S and S' denote placement into the level schemes of Figs. 4 and 5, respectively; and d denotes double placement.

E_γ (keV)	I_γ (relative)		$\alpha_k \times 10^3$	ICC measurements Multipolarity of γ ray	Previous results	Coincident γ rays (keV)
92.23(4)	178(10)	S				224, 307, 338, 410, 534, 545, 562, 1317, 1483
93.88(3)	48(5)	S				
95.2(4)	weak	N				298
100.3(4)	26(2)	S'			$M1,E2$ [5]	192, 215, 298, 317, 330, 349, 426, 542, 968
103.01(2)	529(17)	S	499(15)	$M1$		157, 208, 294, 307, 338, 352, 363, 379, 387, 432, 471, 551, 572, 581, 590, 621, 629, 712, 753, 778, 1398
108.47(3)	5.7(9)	S				
127.3(2)	5.3(12)	S',N				298
151.7(3)	2.9(7)	N				
157.60(3)	391(11)	S	150.2(45)	$M1$		103, 208, 224, 352, 379, 387, 432, 455, 491, 595, 753, 823, 870, 897, 942
162.6(1)	4.9(7)	N				
189.2(4)	weak	S,N				546
192.50(3)	36.5(12)	S'	27.0(27)	$E1$	$M1,E2$ [5] $\Delta I=0$, $E1+M2$ [6]	100, 215, 317, 349, (352), 411, 560, 700, 775
208.09(2)	172.6(48)	S	90(20)	$M1,E2$		103, 157, 224.5, 352, 379, 387, 455, 491, 612, 753, 791, 858, 1153
215.02(2)	38.0(12)	S'	83.3(31)	$M1+E2$	$M1,E2$ [5] $M1(+E2)$ [6]	100, 192, 298, 317, 335, 349, 382, 426, 542, 642, 669, 775, 968, 1068
224.14(2)	50.8(18)	S	58.1(27)	$M1$		93, 307, 321, 338, 410, (503)
224.5(5)		S,N		$(M1)$		157, 208, 352
274.5(4)	weak	S',N				192, 324, 365, 542, 775, 968
287.8(1)	6.5(9)	N				410, 426
293.95(9)	20.1(8)	S	28.9(66)	$M1,E2$		377, 551
298.53(2)	309.2(83)	S'	32.2(9)	$E2$	$E2$ [5]	95, 127, 192, 215, 317, (349), 352, 378, 473, 482, 586, 628, 669, 783, 848, 885, 976, 1022, 1377
302.4(4)	weak	S,N				
307.79(3)	105.2(24)	S	28.6(22)	$E2,(M1)$		92, 103, 224, 338, (470), (545), (562), 626
317.04(5)	15.7(21)				$M1,E2$ [5] $M1(+E2)$ [6]	100, 192, 215, 298, 321, 352, 382, 426, 542, 642, 775, 968, 1283
321.41(5)	18.0(10)	S,N	21.5(39)	$M1,E2$		224, 338, 410, (562), (854)
324.25(5)	18.8(14)	N	21.8(46)	$M1,E2$		274, 349, 365, 374, 411, 426, 467, 775, 1167

TABLE I. (*Continued*).

E_γ (keV)	I_γ (relative)	$\alpha_k \times 10^3$	ICC measurements Multipolarity of γ ray	Previous results	Coincident γ rays (keV)
330.9(1)	4.6(7) S',N,d				100
335.6(4)	weak N				215
338.01(1)	232.2(43) S	21.4(5)	$M1,(E2)$		92, 103, 224.1, 307, 321, (365), 410, 503,
					545, 771, 813, 854, 980, 1039
341.34(3)	70.3(15) S	18.2(10)	$M1,E2$		735, 950, 988
346.1(2)	8(1) S',N				426
349.66(8)	66.8(15) S'	5.1(10)	$E1$	$M1,E2$ [5]	(95), 100, (127), 192, 215, 298, 317, 324,
				$M1+E2$ [6]	365, 391, 405, 411, 426, 467, 802
352.0(4)	< 100			$M1,E2$ [5]	192, 215, 317, 382, 542, 775, 968
				$M1(+E2)$ [6]	
352.16(2)	415(13) S	5.45(51)	$E1$		103, 157, 208, 224, 365.5, 379, 387, 432,
					491, 529, 590, 595, 753, 823, 831, 870,
					897, 939, 942, 952, 1101
363.06(2)	160.3(33) S	15.3(18)	$M1,E2$		103, 482, 621, 630, (672), 919
365.1(4) }	11.0(9) N				324, 374, 426, 467, 775
365.5(1) }	S,N				(338), 352
374.56(5)	7.8(16) N				324, 365
377.34(6)	11.5(7)				293, 402, 410, 537
378.9(2) }	N				298
379.09(5) }	23.0(9) S,N				157, 208, 352, (365), 455
382.3(3)	weak			$M1,E2$ [5]	215, 317, 352, 968
				$M1(+E2)$ [6]	
387.18(5)	15.4(7) S,N				157, 208, 352, (365)
391.60(5)	20.1(8)				349, 405, 411, 426, (700), 775
401.9(2)	15.9(8) S,N				377, 546
404.27(3)	18.6(9) S				411
405.3(3)	N				349, 391, 411, 426, 775, 802
410.91(3) }	100(22) S	11.7(10)	$M1,E2$		92, 224, 321, 338, 377, 404, 411, 470,
					534, 537, 545, 562, (621), 626, 654, 700,
					771, 801, 813, 926, 944, 979, 1136, 1147,
					1167, 1173, 1238, 1317, 1328, 1352, 1470
411.2(2) }	S'				192, 324, 349, 410, 426, 700, 775
424.20(3)	106.2(24) S				479, (816), (867), 1012
426.13(2)	369.8(83) S'	10.58(46)	$M1,E2$	$M1,E2$ [5]	100, 192, 215, 317, 324, 346, 349, 365,
				$M1(+E2)$ [6]	391, 411, 458, 467, 479, 498, 542, 560,
					642, 663, 684, 758, 860, 875, 978, 1224,
432.51(4)	24(2) S				103, 157, 352, 455, 551
447.83(6)	4.3(6) S	9.7(51)	$M1,E2$		
455.19(7)	115.1(20) S	2.95(46)	$E1$		157, 208, 432, 590, 595, 791, 939

TABLE I. (*Continued*).

E_γ (keV)	I_γ (relative)		$\alpha_k \times 10^3$	ICC measurements Multipolarity of γ ray	Previous results	Coincident γ rays (keV)
457.01(2)	19.9(9)	S				
458.64(6)	22.7(11)	S',N	8.1(15)	$M1,E2$		426
466.11(5)	29.3(13)	S	7.9(15)	$M1,E2$		
467.24(5)	15.0(13)	S'			$E2$ [5]	(127), 298, 324, 349, 365, 374, (410), 426,
					$\Delta I=0,2$ [6]	(700), 775
470.79(4)	21.0(8)	S	8.5(16)	$M1,E2$		410
471.62(6)	weak	S				103
473.63(3)	36.5(10)	S',N	8.5(9)	$M1,E2$		298
476.59(5)	19.7(9)	S,N	7.2(15)	$M1,E2$		735
479.9(2)	78.1(71)	S',d				424, 426, 518, 654
480.2(4)	45.8(62)				$M1,E2$ [5]	498
			7.8(12)	$(M1,E2)$	$\Delta I=1$ [6]	
480.8(4)		S				762
482.3(1)	9.8(7)	S',d				298, 363
484.6(1)		S,N				551
491.45(7)	42.6(12)	S,N,d	6.99(74)	$(M1,E2)$		103, 157, 208, 352, 365, 546, 725
498.2(2)	5.6(10)	S',N	8.7(43)	$M1,E2$		426, 480
503.2(1)	6.9(10)	S,N				
518.04(3)	34.3(12)	S	1.81(54)	$E1$		480, 654, (1012)
529.4(1)	10.3(9)	N				352, 590
534.49(6)	9.1(9)	S,N	6.0(33)	$M1,E2$		92, 410
537.43(5)	14.2(9)	S,N				377, 410
542.4(2)	15.2(43)	S'				215, 317, 426
545.4(2)		S,N				92, 307, 338, 410, (845)
546.33(6)	215.9(52)	S	6.6(10)	$M1,(E2)$		189, 402, 491, 665, 1010
550.83(7)	98(13)	S	5.4(61)	$(M1,E2)$		330, 950
551.4(1)	98(10)	S				103, 293, 484, 571, 633
558.4(1)	7.3(9)	N				
560.9(1)	11.8(12)	N				192, 426, 968
562.27(5)	36.7(14)	S,N	5.33(70)	$M1,E2$		92, 307, 321, 410
571.80(6)	15.7(24)	S,N				103, 551
574.5(1)	8.2(9)	S				(762)
586.0(4)	6.0(20)	S',N				298
587.7(2)	5.0(20)	N				(410)
590.22(3)	54.3(17)	S	4.84(43)	$M1,(E2)$		103, 352, 455, 529
595.5(3)	<29	S,N	5.02(60)	$(M1,E2)$		103, 157, 352, 455, 612
602.8(2)	6.4(12)	N				
612.89(5)	28.8(10)	S,N	1.47(89)	$E1$		208, (432)
621.47(5)	20.1(9)	S	5.4(11)	$M1$		103, 363, (410)

TABLE I. (*Continued*).

E_γ (keV)	I_γ (relative)	$\alpha_k \times 10^3$	ICC measurements Multipolarity of γ ray	Previous results	Coincident γ rays (keV)
624.3(4)	weak *N*				752
626.8(1)	45.5(13) *S*,*N*				103, 307, 410, 725
628.66(3) }					298
630.0(1) }	20.9(10) *S*,*N*				103, 365
633.5(1)	9.9(9) *N*				551
635.5(1)	8.4(9) *N*				
642.59(7)	15.8(13) *S*′	3.7(10)	*M*1,*E*2	*M*1,*E*2 [5]	215, 317, 349, (3520), 426, 775
646.4(4)	weak *S*′			*M*2 [5]	(752)
				*M*2 [6]	
654.60(5)	24.6(10) *S*,*N*	4.3(9)	(*M*1,*E*2)		410, 424, 480, 518, (587)
663.86(5)	24.6(11) *S*′,*N*	2.89(30)	*E*2		426
665.8(1)	9.4(10) *S*,*N*				546
669.86(5)	19.3(10) *S*′	2.59(67)	*E*2,(*M*1)		100, 215, 298, 317, (352), (382)
672.6(2)	3.5(10) *S*,*N*				
676.1(2)	4.8(9) *N*				
681.5(3)	5.2(13) *N*				
684.11(6)	15.4(10) *S*′,*N*	4.1(11)	*M*1,(*E*2)		426
700.73(9)	13.7(10) *N*	2.22(88)	(*M*1,)*E*2		192, (391), 410, 467, 802
705.2	10(5) *S*				(424), (518)
712.07(4)	31.6(12) *S*	2.31(40)	*E*2,(*M*1)		103
725.2(2)	9.6(14) *N*				491, 626
735.42(3)	215.6(81) *S*	2.58(33)	*M*1,*E*2		302, 341, 476, 988, 1180
752.78(3)	63.2(86) *S*′	3.26(47)	*M*1	*M*1,*E*2 [5]	624, 646, 1021, 1248
				*M*1+*E*2 [6]	
753.9(5)	weak *N*				103, 157, 208, 352, 455
758.0(4)	weak *N*				426
762.0(1)	6.8(10) *S*,*N*				481
771.0(4)	10.2(10) *N*				338
775.87(2)	127.1(50) *S*′	0.93(23)	*E*1	*M*1,*E*2 [5]	(100), 192, 215, 274, 317, 324, 352, (365),
				*E*1 [6]	391, 405, 411, 467, (642), (802)
778.59(3)	22.1(14) *S*				103
782.6(1)	9.2(15) *N*				
783.6(4)	weak *N*				298
784.1(3)	5.3(14) *N*				
785.7(2)	5.6(10) *S*				
791.6(2)	8.7(11) *N*				
801.2(2)	8.9(14) *S*,*N*				410
802.9(4)	5.9(14) *N*				349, 405, 426, (700), 775
813.8(2)	6.6(11) *N*				338, 410

TABLE I. (*Continued*).

E_γ (keV)	I_γ (relative)	ICC measurements $\alpha_k \times 10^3$	ICC measurements Multipolarity of γ ray	Previous results	Coincident γ rays (keV)
815.3	8.5(11) *S*				
823.4(1)	15.4(16) *S,N*				157, 352
831.4(3)	3.7(12) *N*				352
836.6(1)	10.7(31) *N*				(410)
845.0(4)	weak *N*				338, (410)
848.5(3)	9.2(16) *N*				298
858.2(3)	5.7(11) *N*				157, 208
860.5(2)	weak *N*				426
867.7(1)	10.3(11) *S*				(424)
870.5(1)	33.7(18) *S*	1.75(36)	*M*1,*E*2		103, 157, 352, 455, (612)
874.7(1)	<5				
875.8(1)	17.9(18) *S′,N*	1.45(53)	*M*1,*E*2		426
885.3(4)	weak *N*				298
893.2(2)	5.2(10) *N*				
897.3(1)	16.2(12) *N*	1.84(73)	*M*1,*E*2		103, 157, 352
906.1(1)	11.3(12) *S′*				
908.9(2)	6.7(17) *N*				
917.82(8)	5.0(13) *S*				
919.4(2)	weak *N*				363
926.9(4)	8.8(13) *S,N*				410
939.3(2)	weak *N*				103, 352, 455
942.2(1)	12.3(19) *N*				157, 352
944.0(4)	weak *N*				410
948.28(6)	23.4(17) *S*	1.13(38)	*E*2,(*M*1)		
950.6(2)	6.2(14) *N*				341, 735
952.7(1)	14.9(15) *S,N*				(103), 352
968.47(2)	102.4(47) *S′*	1.38(12)	*E*2,(*M*1)	*M*1,*E*2 [5] *M*1(+*E*2) [6]	100, 215, 274, 317, 352, 382, 560
976.47(7)	15.6(14) *S′,N*				298
978.3(4)	weak *N*				426
979.6(1)	6.8(13) *N*				338, 410
988.6(4)	weak *N*				341, 735
1010.1(2)	7.5(12) *N*				546
1012.7(1)	15.7(16) *N*				424, 518
1021.3(4)	weak				752
1022.1(1)	11.4(14) *S′,N*				298
1038.8(2)	13.6(20) *N*				338, 410
1068.4(4)	weak *S′*				215, 317, 352
1087.4(1)	19.2(38) *S,N*				

TABLE I. (*Continued*).

E_γ (keV)	I_γ (relative)		$\alpha_k \times 10^3$	ICC measurements Multipolarity of γ ray	Previous results	Coincident γ rays (keV)
1101.4(2)	8.7(14)	*N*				
1109.8(1)	16.8(16)	*N*	1.02(35)	$M1,E2$		
1122.26(5)	50.8(26)	*S,N*	0.97(13)	$E2,(M1)$		
1129.3(1)	<11	*S*				
1136.6(4)	weak	*N*				410
1138.8(1)	28.4(16)	*S,N*	0.83(17)	$E2,(M1)$		
1147.5(2)	9.0(12)	*N*	1.11(62)	$M1,E2$		307, 410
1153.4(4)	weak	*N*				208, 352
1167.7(4)	weak	*N*				307, 324, 410
1173.3(1)	weak	*N*				410
1180.0(5)	weak	*N*				735
1212.1(1)	13.7(13)	*S,N*	0.70(32)	$(M1,E2)$		
1224.2(2)	4.9(22)	*N*				298, 426
1238.3(4)	weak	*N*				410
1248.2(3)	weak					752
1258.8(2)	9.9(12)	*N*				410
1283.8(4)	weak	*S'*			$\Delta I=1$ [6]	
1317.3(3)	12.1(16)	*N*				92, 307, 410
1328.1(4)	weak	*N*				
1351.6(2)	5.2(28)	*N*				410
1377.9(1)	19.6(14)	*N*				298
1398.3(4) }		*N*				103
1398.9(4) }	12.4(13)	*S'*			$E3$ [5] $E3$ [6]	
1470.1(4)	weak	*N*				410
1483.4(4)	weak	*N*				92, 410

The Hamiltonian of the interacting-boson-fermion-fermion model is [18]

$$H_{\mathrm{IBFFM}} = H_{\mathrm{IBFM}}(\pi) + H_{\mathrm{IBFM}}(\nu) - H_{\mathrm{IBM}} + H_{\mathrm{eff}} \ ,$$

where $H_{\mathrm{IBFM}}(\pi)$ and $H_{\mathrm{IBFM}}(\nu)$ denote the IBFM Hamiltonians for the neighboring odd-even nuclei with an odd proton and odd neutron, respectively [19]. H_{IBM} denotes the IBM Hamiltonian [20] for the even-even core nucleus. H_{eff} denotes the residual proton-neutron interaction. Depending on whether one uses the Schwinger or the Holstein-Primakoff representation of the SU(6) boson Hamiltonian, one can distinguish between the interacting-boson-fermion-fermion and the odd-odd truncated-quadrupole-phonon representations, respectively [21]. The two representations are equivalent on the phenomenological level.

The IBFFM Hamiltonian was diagonalized in the proton-neutron-boson basis:

$$|(j_\pi, j_\nu) I_{\pi\nu}, n_d R; J\rangle \ ,$$

where j_π and j_ν stand for the proton and neutron angular momenta coupled to $I_{\pi\nu}$, n_d is the number of d bosons, R is their total angular momentum, and J is the spin of the state. The computer code IBFFM, used for the calculations, was written by Brant, Paar, and Vretenar [22].

The boson core has been treated in the SU(5) limit of IBM (corresponding to the harmonic vibrations). This is an acceptable approach in the case of spherical nuclei like even-even Sn isotopes, if we want to describe only low-energy states, because the contribution of two- (and higher-) d-boson components is small. We used $\hbar\omega_2 = 1.3$ MeV effective phonon energy, which is the energy of the 2_1^+ state of ^{114}Sn.

Since we are considering the low-lying states in a nearly spherical nucleus, we use the reduced total boson number $N_{\max} = 2$. This strongly reduces the scope of computations, without sizable effect on the properties of the

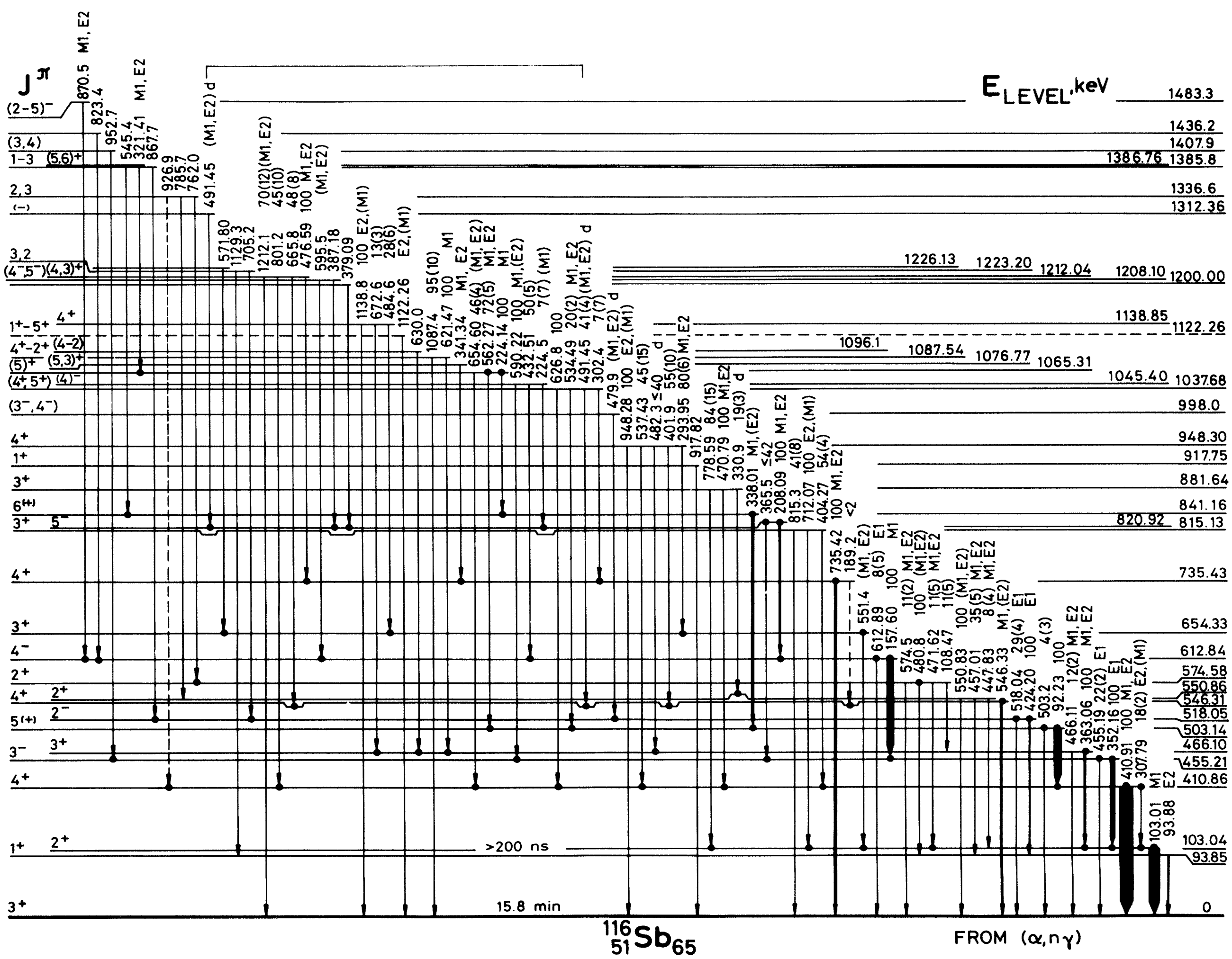

FIG. 4. Proposed low-spin (≲6) level scheme of ^{116}Sb (based on the 3^+ ground state) from ^{113}In$(\alpha,n\gamma)^{116}$Sb reaction. Solid circles at the ends of arrows indicate $\gamma\gamma$-coincidence relations. γ-ray branching ratios and multipolarities are also given. d denotes double placement.

low-lying states. Even the two-d-boson components had little effect on the wave functions of the states below 1200 keV (see Table III).

The calculations were performed for the low-lying positive parity states. The shell-model space consisted of the $2d_{5/2}, 1g_{7/2}, 3s_{1/2}, 2d_{3/2}$ subshells for the proton particle and neutron quasiparticles.

The occupation probabilities for neutrons were taken from the systematics of the available data (for citations see Ref. [21]): $V^2(\nu d_{5/2})=0.88$, $V^2(\nu g_{7/2})=0.72$, $V^2(\nu s_{1/2})=0.23$, $V^2(\nu d_{3/2})=0.20$. The calculations were performed with two sets of the proton single-particle and neutron quasiparticle energies, strength parameters of the fermion-boson interaction, and parameters of the residual interaction and effective charges. They are given in Table II.

In the set 1 calculation, the single-proton and the quasineutron energies were adjusted to the energy spectrum of ^{116}Sb. The single-proton energies obtained in this way are close to the values used by Pinho *et al.* [23] and

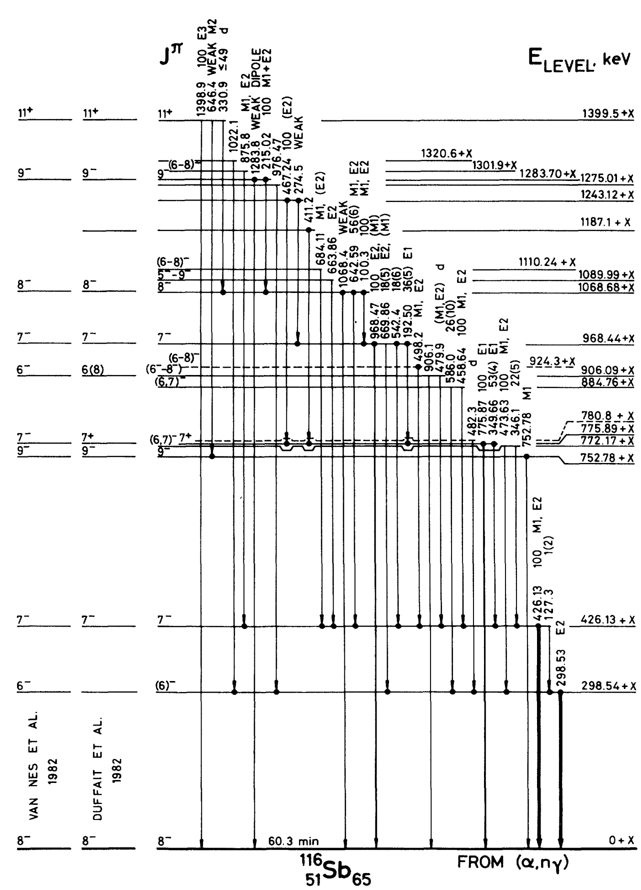

FIG. 5. Proposed high-spin ($\gtrsim 6$) level scheme of ^{116}Sb (based on the 60.3-min 8^- isomeric state) from ^{113}In$(\alpha,n\gamma)^{116}$Sb reaction. Solid circles at the ends of arrows indicate $\gamma\gamma$-coincidence relations. γ-ray branching ratios and multipolarities are also given. Former results (Refs. [5] and [6]) are shown on the left side. d denotes double placement.

Goldstein *et al.* [24] for the description of the ^{115}Sb levels. The neutron quasiparticle energies are close to the energies of the corresponding ^{115}Sn states.

The strength parameters of the boson-fermion dynamical and exchange interactions were as follows: $\Gamma_0^p=1.0$ MeV, $\Lambda_0^p=0$ MeV, respectively. These values are close to the values which correspond to the IBFM [19] description of the energy levels and electromagnetic moments of ^{115}Sb. $\Lambda_0^p=0$ MeV is a reasonable value, taking into account that the phonon consists mainly of neutron excitations. We note that the values of Γ_0^p and Λ_0^p used here for ^{116}Sb are similar to those which have been employed previously for the IBFFM description of the odd-odd In energy spectra [25].

The strength parameters of the boson-fermion interaction were $\Gamma_0^n=0.7$ MeV and $\Lambda_0^n=2.3$ MeV. These values have been adjusted in IBFM to the energy spectrum and electromagnetic moments of ^{115}Sn.

In the set 1 calculations, the residual interaction has the following form: $H_{\text{eff}}=4\pi\delta(\mathbf{r}_p-=\mathbf{r}_n)\times[v_D+v_S\boldsymbol{\sigma}_p\cdot\boldsymbol{\sigma}_n]+V_{\sigma\sigma}(\boldsymbol{\sigma}_p\cdot\boldsymbol{\sigma}_n)$. Here v_D and v_S are the parameters of the Wigner and Bartlett forces, δ is the Dirac symbol, $\mathbf{r}_p$ and $\mathbf{r}_n$ are the position vectors of the proton and neutron, respectively, $\boldsymbol{\sigma}$'s are the Pauli spin matrices, and $V_{\sigma\sigma}$ is the parameter of spin-spin interaction.

The strength of the residual force were adjusted to the energy spectrum and electromagnetic properties of ^{116}Sb. $V_{\sigma\sigma}$ is close to the standard estimate: $\approx 15/A \approx 0.13$. The v_D/v_S ratio is the same as in the case of odd-odd In nuclei [25].

In the set 2 calculations, the proton single-particle and neutron quasiparticle energies were first fitted to the ^{115}Sb and ^{115}Sn nuclei, respectively, and then adjusted to ^{116}Sb by allowing up to 100 keV deviations from these values. The strength parameters of the boson-fermion interaction together with the single (quasi)particle energies were adjusted to the energies and electromagnetic properties of the ^{115}Sb and ^{115}Sn using the IBFM calculations. The residual interaction has the following form in the set 2 calculations: $H_{\text{eff}}=V_0\delta(\mathbf{r}_p-\mathbf{r}_n)(1+\alpha\sigma_p\sigma_n)$. The strength of the δ force was fitted to the energy spectrum of ^{116}Sb. The $V_0=360$ MeV fm^3 value is about $\frac{3}{4}$ of the value characteristic for the double magic region. The radial matrix elements of the interaction were calculated using harmonic oscillator wave functions with the oscillator parameter $b=2.253$ fm. The $\alpha=0.2$ value, used in the calculations, is in agreement with the corresponding one in the double magic region.

Using the wave functions obtained by diagonalization, we have calculated the electromagnetic properties. The effective charges and gyromagnetic ratios were close to the standard values in both sets of calculations:

$$e^p=1.5e,\ e^n=0.5e,\ g_l^p=1,\ g_l^n=0,\ g_s^p=0.65g_s^p(\text{free}),$$

$$g_s^n=0.5g_s^n(\text{free}),\ g_R=Z/A\approx 0.4397 .$$

The experimental and theoretical level energies of the low-lying positive-parity states of ^{116}Sb are shown in Fig. 6.

TABLE II. Parameters of the IBFFM calculations.

Parameters		Set I	Set II
Proton single-particle energies (MeV)	$\epsilon(\pi g\frac{7}{2})-\epsilon(\pi d\frac{5}{2})$	0.85	0.68
	$\epsilon(\pi d\frac{3}{2})-\epsilon(\pi d\frac{5}{2})$	2.0	1.45
	$\epsilon(\pi s\frac{1}{2})-\epsilon(\pi d\frac{5}{2})$	2.65	1.62
Quasineutron energies (MeV)	$E(\nu g\frac{7}{2})-E(\nu s\frac{1}{2})$	0.45	0.25
	$E(\nu d\frac{5}{2})-E(\nu s\frac{1}{2})$	0.80	0.60
	$E(\nu d\frac{3}{2})-E(\nu s\frac{1}{2})$	0.47	0.71
Strength parameters of the nucleon-core interaction (MeV)	Γ_0^p	1.0	0.53
	Λ_0^p	0	0
	Γ_0^n	0.7	1.414
	Λ_0^n	2.3	1.30
Parameters of the residual interaction	v_D MeV	-0.6	
	v_S MeV	-0.15	
	$V_{\sigma\sigma}$ MeV	0.11	
	V_0 MeV fm^3		360
	α		0.2
	b fm		2.253
Effective charge of vibration	e^{vibr}	$1.8e$	$2.0e$

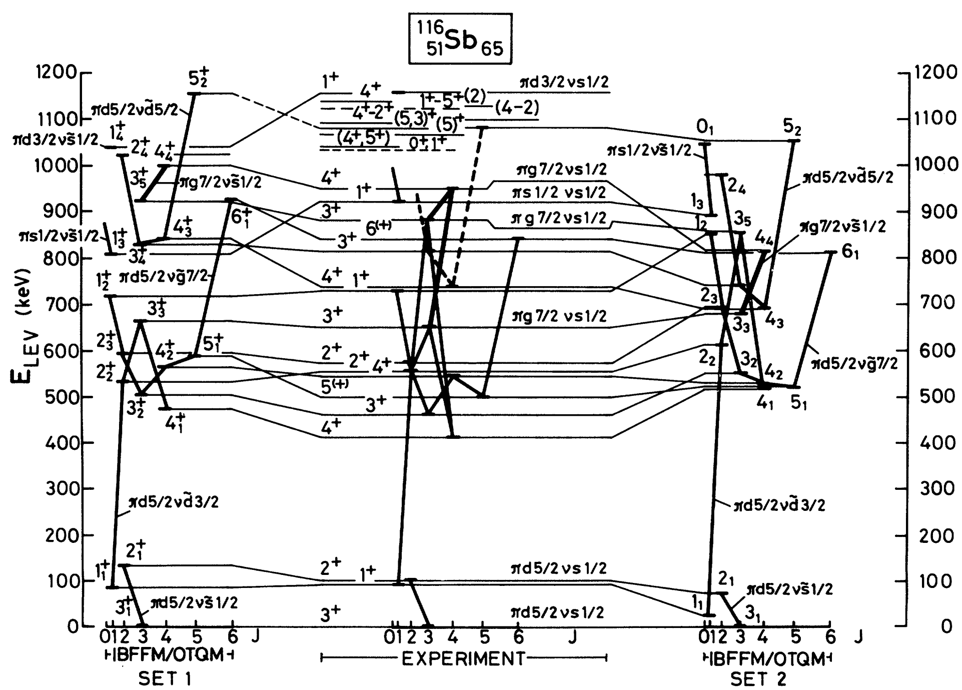

FIG. 6. IBFFM energy spectrum of ^{116}Sb in comparison with experimental data. The solid lines connect the members of the given multiplet. The leading proton-neutron configurations for several multiplets were identified on the basis of the ($^3He,d$) proton transfer results [4].

TABLE III. Wave functions of some low-lying states of ^{116}Sb. For the given J^{π} state the $|(j_p j_n)I;NR\rangle$ wave-function components and the corresponding amplitudes are given. Only components with larger than 10% weight are given.

J^{π}	Set 1		Set 2	
1_1^+	$(\frac{5}{2},\frac{3}{2})1;00$	0.802	$(\frac{5}{2},\frac{3}{2})1;00$	−0.762
			$(\frac{1}{2},\frac{1}{2})1;00$	0.372
1_2^+	$(\frac{5}{2},\frac{7}{2})1;00$	0.762	$(\frac{5}{2},\frac{7}{2})1;00$	−0.848
	$(\frac{5}{2},\frac{7}{2})3;12$	−0.423		
1_3^+	$(\frac{1}{2},\frac{1}{2})1;00$	0.540	$(\frac{1}{2},\frac{1}{2})1;00$	−0.580
	$(\frac{5}{2},\frac{1}{2})3;12$	0.540	$(\frac{5}{2},\frac{3}{2})1;00$	−0.364
			$(\frac{5}{2},\frac{1}{2})2;12$	−0.330
			$(\frac{5}{2},\frac{7}{2})1;00$	−0.324
2_1^+	$(\frac{5}{2},\frac{1}{2})2;00$	0.726	$(\frac{5}{2},\frac{1}{2});00$	−0.851
	$(\frac{5}{2},\frac{3}{2})2;00$	−0.329		
2_2^+	$(\frac{5}{2},\frac{3}{2})2;00$	0.581	$(\frac{5}{2},\frac{3}{2})2;00$	0.770
	$(\frac{5}{2},\frac{7}{2})2;00$	−0.499		
2_3^+	$(\frac{5}{2},\frac{7}{2})2;00$	−0.607	$(\frac{5}{2},\frac{7}{2})2;00$	−0.830
	$(\frac{5}{2},\frac{3}{2})2;00$	−0.472		
	$(\frac{5}{2},\frac{1}{2})2;00$	−0.324		
3_1^+	$(\frac{5}{2},\frac{1}{2})3;00$	−0.836	$(\frac{5}{2},\frac{1}{2})3;00$	0.881
	$(\frac{5}{2},\frac{1}{2})3;12$	0.345		
3_2^+	$(\frac{5}{2},\frac{7}{2})3;00$	−0.783	$(\frac{5}{2},\frac{7}{2})3;00$	−0.860
3_3^+	$(\frac{5}{2},\frac{3}{2})3;00$	−0.716	$(\frac{7}{2},\frac{1}{2})3;00$	0.672
	$(\frac{7}{2},\frac{1}{2})3;00$	0.325	$(\frac{5}{2},\frac{3}{2})3;00$	−0.490
3_4^+	$(\frac{5}{2},\frac{5}{2})3;00$	−0.714	$(\frac{5}{2},\frac{5}{2})3;00$	−0.798
	$(\frac{5}{2},\frac{5}{2})4;12$	−0.467	$(\frac{5}{2},\frac{5}{2})4;12$	−0.394
3_5^+	$(\frac{7}{2},\frac{1}{2})3;00$	−0.687	$(\frac{5}{2},\frac{3}{2})3;00$	−0.678
	$(\frac{5}{2},\frac{3}{2})3;00$	−0.408	$(\frac{7}{2},\frac{1}{2})3;00$	−0.532
4_1^+	$(\frac{5}{2},\frac{3}{2})4;00$	−0.794	$(\frac{5}{2},\frac{3}{2})4;00$	0.787
	$(\frac{5}{2},\frac{3}{2})4;12$	0.406		
4_2^+	$(\frac{5}{2},\frac{7}{2})4;00$	−0.818	$(\frac{5}{2},\frac{7}{2})4;00$	0.850
	$(\frac{5}{2},\frac{7}{2})5;12$	−0.383	$(\frac{5}{2},\frac{7}{2})5;12$	0.332
4_3^+	$(\frac{5}{2},\frac{5}{2})4;00$	−0.764	$(\frac{5}{2},\frac{5}{2})4;00$	−0.781
	$(\frac{5}{2},\frac{5}{2})5;12$	−0.381		
4_4^+	$(\frac{7}{2},\frac{1}{2})4;00$	−0.786	$(\frac{7}{2},\frac{1}{2})4.00$	0.844
	$(\frac{7}{2},\frac{1}{2})4;12$	0.351		
5_1^+	$(\frac{5}{2},\frac{7}{2})5;00$	0.825	$(\frac{5}{2},\frac{7}{2})5;00$	−0.889
	$(\frac{5}{2},\frac{7}{2})6;12$	0.391		
6_1^+	$(\frac{5}{2},\frac{7}{2})6;00$	0.867	$(\frac{5}{2},\frac{7}{2})6;00$	−0.913
	$(\frac{5}{2},\frac{7}{2})5;12$	−0.355	$(\frac{5}{2},\frac{7}{2})5;12$	0.332

The wave functions of the low-lying states are shown in Table III. From dominant components in the wave functions we see that the IBFFM/OTQM calculation preserves the approximate classification of the parabolic rule [26], which is given in [14]. In set 1 calculations, the 2_1^+, 3_1^+ states are dominated with $\pi d_{5/2}\nu\tilde{s}_{1/2}$, the 1_1^+, 2_2^+, 3_3^+, 4_1^+ states with $\pi d_{5/2}\nu\tilde{d}_{3/2}$, the 1_2^+, 2_3^+, 3_2^+, 4_2^+, 5_1^+, 6_1^+ states with $\pi d_{5/2}\nu\tilde{g}_{7/2}$, the 3_4^+, 4_3^+, 5_2^+ states with $\pi d_{5/2}\nu\tilde{d}_{5/2}$, and the 3_5^+, 4_4^+ states with $\pi g_{7/2}\nu\tilde{s}_{1/2}$ proton-neutron multiplet components. In the set 2 calculations, the situation is very similar, but the main components of the 3_3 and 3_5 states have $\pi g_{7/2}\nu\tilde{s}_{1/2}$ and $\pi d_{5/2}\nu\tilde{d}_{3/2}$ configurations, respectively. It is obvious that the $\pi g_{7/2}\nu\tilde{s}_{1/2}$ and $\pi d_{5/2}\nu\tilde{d}_{3/2}$ components are strongly mixed in the 3_3 and 3_5 states.

The nearly parabolic feature of the E vs $J(J+1)$ plot of the $\pi d_{5/2}\nu\tilde{d}_{3/2}$, $\pi d_{5/2}\nu\tilde{d}_{5/2}$, and $\pi d_{5/2}\nu\tilde{g}_{7/2}$ multiplets are approximately reproduced. The energy splittings of the $\pi d_{5/2}\nu\tilde{s}_{1/2}$ and $\pi g_{7/2}\nu\tilde{s}_{1/2}$ doublets agree well with the experimental data.

The known magnetic dipole moments of the ^{116}Sb states are summarized in Table IV. The experimental and the IBFFM magnetic dipole moments agree very well. The IBFFM calculations show that the contribution of the collective $M1$ operator to the magnetic moment is small. This can provide an explanation of why the simple additivity relation predicts the magnetic moment of the 3_1^+ ground state rather well.

The calculated electric quadrupole moment of the 3_1^+ ground state is -0.47 eb (set 1). The corresponding experimental value is not yet known, but the quadrupole moment of the $\frac{5}{2}^+$ ground state in the neighboring ^{115}Sb nucleus is rather close to this result: $Q=-0.36(6)$ eb [27].

The $E2/M1$ mixing ratios and the γ branching ratios of the low-lying states in ^{116}Sn are given in Table V. As seen, the experimental branching ratios are reproduced within a factor of $\lesssim 6$ (with two exceptions). In the majority of cases the theoretical $E2/M1$ mixing ratios agree with the experimental ones within the error limits.

TABLE IV. Magnetic dipole moments (μ in μ_N) of some ^{116}Sb states. IBFFM subscript indicates the results of the present calculations.

	^{116}Sb states	
Magnetic dipole moment	3_1^+ ground 15.8 min	1_1^+, 94 keV >200 ns
μ_{exp}	$\lvert\mu_{\mathrm{exp}}\rvert=2.715(9)$[a]	+2.47(9)[b]
μ_{emp}	+2.66(1)[a,c]	
μ_{IBFFM} set 1	+2.79	+2.30
μ_{IBFFM} set 2	+2.88	+2.18

[a]Reference [9].
[b]Reference [10].
[c]Reference [9]; the empirical value was calculated supposing $[\pi d_{5/2}\nu s_{1/2}]_{3^+}$ configuration and also taking into account collective correction.

TABLE V. Transitions within the low-lying ^{116}Sb states.

Experimental data								IBFFM/OTQM calc.			
								Set 1		Set 2	
E_i (keV)	J_i^π	E_f (keV)	J_f^π	E_γ (keV)	Multipolarity	δ	I_γ	$\lvert\delta\rvert$	I_γ	$\lvert\delta\rvert$	I_γ
103	2_1^+	0	3_1^+	103	$M1$	$-0.02(14)$		0.012		0.01	
411	4_1^+	0	3_1^+	411	$M1,E2$	$+2.1^{+1.1}_{-1.3}$	100	0.6	100	1.42	100
		103	2_1^+	308	$E2$		18(2)	∞	23	∞	61
466	3_2^+	103	2_1^+	363	$M1,E2$	$-0.02(8)$	100	0	100	0.02	100
		0	3_1^+	466	$M1,E2$	$-0.27(20)$	12(2)	0.17	16	0.18	5
546	4_2^+	0	3_1^+	546	$M1,(E2)$	$+0.07(8)$		0.58		1.02	
551	2_2^+	0	3_1^+	551	$(M1,E2)$	>0.3	100	0.01	100	0.09	100
		94	1_1^+	457	$M1,E2$	$-0.16^{+0.14}_{-0.24}$	35(5)	0.11	46	0.11	80
		103	2_1^+	448	$M1,E2$	$-0.28^{+0.28}_{-0.39}$	8(4)	0.04	9	0.07	4
575	2_3^+	0	3_1^+	575	$M1,E2$	$+0.25^{+0.63}_{-0.33}$	11(2)	0.01	276	0.11	53
		94	1_1^+	481	$(M1,E2)$	$-0.8^{+0.9}_{-1.1}$	100	0.11	100	0.06	100
		103	2_1^+	472	$M1,E2$		11(5)	0.04	68	0.09	2
		466	3_2^+	108		$0.00^{+0.35}_{-0.42}$	11(5)	0.003	8	0.01	45
654	3_3^+	0	3_1^+	654	$(M1,E2)$	$-0.49^{+0.19}_{-0.25}$	14(10)	0.82	3	28.2	11
		103	2_1^+	551	$(M1,E2)$		100	0.18	100	0.37	100
732	1_2^+	94	1_1^+	638	$M1,E2$	$-0.45^{+0.12}_{-0.17}$	25(10)	0.75	5	4.10	4
		103	2_1^+	629			100	0.13	100	0.16	100
		551	2_2^+	181	$M1,E2$		7(3)	<0.01	18	<0.01	16
		575	2_3^+	157			14(10)	<0.01	14	<0.01	45
735	4_3^+	0	3_1^+	735	$M1,E2$	$-0.22(12)$		0.03		0.45	
815	3_4^+	0	3_1^+	815		$-0.09(21)$	41(8)	0.07	132	3.27	1
		103	2_1^+	712	$E2,(M1)$	0.00(63)	100	0.08	100	0.03	100
		411	4_1^+	404		$-0.12(13)$	54(4)	0.07	154	0.05	125
841	$6_1^{(+)}$	503	$5_1^{(+)}$	338	$M1,(E2)$	$+0.09(16)$		0.09		0.08	
882	3_5^+	103	2_1^+	779		$-0.13(15)$	84(15)	0.07	7000	0.12	128
		411	4_1^+	471	$M1,E2$		100	0.28	100	0.02	100
		551	2_2^+	331			19(3)	0.10	50	0.02	51
918	1_3^+	0	3_1^+	918			100	∞	100		100
		94	1_1^+	824			81(5)	0.23	38		745
		551	2_2^+	367			93(4)	0.1	28		49

ACKNOWLEDGMENTS

We are indebted to Dr. J. Gulyás, Dr. T. Kibédi, Dr. A. Krasznahorkay, Dr. S. Mészáros, Dr. J. Timár, and Dr. A. Valek for their help in the measurements. This work was supported in part by the Hungarian Scientific Research Foundation (OTKA). The financial help of the G. Soros Foundation is also acknowledged.

[1] C. B. Morgan, W. H. Bentley, R. A. Warner, W. H. Kelly, and Wm. C. McHarris, Phys. Rev. C **23**, 1228 (1981).

[2] C. B. Morgan, Ph.D. thesis, Michigan State University, 1975.

[3] R. Kamermans, H. W. Jongsma, T. J. Ketel, R. Van Der Wey, and H. Verheul, Nucl. Phys. **A266**, 346 (1976).

[4] R. Kamermans, J. Van Driel, H. P. Blok, and P. J. Blankert, Phys. Rev. C **17**, 1555 (1978).

[5] P. Van Nes, W. H. A. Hesselink, W. H. Dickhoff, J. J. Van Ruyven, M. J. A. De Voigt, and H. Verheul, Nucl. Phys.

A379, 35 (1982).

[6] R. Duffait, J. Van Maldeghem, A. Charvet, J. Sau, K. Heyde, A. Emsallem, M. Meyer, R. Béraud, J. Tréherne, and J. Genevey, Z. Phys. A **307**, 259 (1982).

[7] J. Blachot and G. Marguier, Nucl. Data Sheets **59**, 333 (1990).

[8] C. Ekström, W. Hogervorst, S. Ingelman, and G. Wannberg, Nucl. Phys. **A226**, 219 (1974).

[9] V. R. Green, C. J. Ashworth, J. Rikovska, T. L. Shaw, N. J. Stone, P. M. Walker, and I. S. Grant, Phys. Lett. B **177**, 159 (1986).

[10] E. A. Ivanov, private communication, cited in P. Raghavan, At. Data Nucl. Data Tables **42**, 189 (1989).

[11] W. F. Van Gunsteren, K. Allaart, and E. Boeker, Nucl. Phys. **A266**, 365 (1976).

[12] J. Van Maldeghem, J. Sau, and K. Heyde, Phys. Lett. B **116**, 387 (1982).

[13] Z. Árvay, T. Fényes, K. Füle, T. Kibédi, S. László, Z. Máté, Gy. Mórik, D. Novák, and F. Tárkányi, Nucl. Instrum. Methods **178**, 85 (1980); T. Kibédi, Z. Gácsi, A. Krasznahorkay, and S. Nagy, ATOMKI Annual Report, Debrecen, 1986, p. 55; T. Kibédi, Z. Gácsi, and A. Krasznahorkay, ATOMKI Annual Report, Debrecen, 1987, p. 100.

[14] Z. Gácsi, T. Fényes, and Zs. Dombrádi, Phys. Rev. C **44**, 626 (1991), the preceding paper.

[15] T. Lönnroth and P. Jauho, Nucl. Instrum. Methods **A261**, 549 (1987).

[16] G. Székely, Comput. Phys. Commun. **34**, 313 (1985).

[17] R. S. Hager and E. C. Seltzer, Nucl. Data Tables A **4**, 1 (1968).

[18] V. Paar, in *In-Beam Nuclear Spectroscopy,* edited by Zs. Dombrádi and T. Fényes (Akad. Kiadó, Budapest, 1984), Vol. 2, p. 675.

[19] F. Iachello and O. Scholten, Phys. Rev. Lett. **43**, 679 (1979); V. Paar, S. Brant, L. F. Canto, G. Leander, and M. Vouk, Nucl. Phys. **A378**, 41 (1982).

[20] D. Janssen, R. V. Jolos, and F. Dönau, Nucl. Phys. **A224**, 93 (1974); A. Arima and F. Iachello, Phys. Rev. Lett. **35**, 1069 (1975).

[21] T. Kibédi, Zs. Dombrádi, T. Fényes, A. Krasznahorkay, J. Tímár, Z. Gácsi, A. Passoja, V. Paar, and D. Vretenar, Phys. Rev. C **37**, 2391 (1988).

[22] S. Brant, V. Paar, and D. Vretenar, computer code IBFFM/OTQM (Institut für Kernphysik, KFA, Jülich, 1985) (unpublished).

[23] A. G. De Pinho and J. M. F. Jeronymo, Nucl. Phys. **A116**, 408 (1968).

[24] I. V. Goldstein and A. G. De Pinho, Z. Naturforsch. **26a**, 1987 (1971).

[25] T. Fényes, Zs. Dombrádi, A. Krasznahorkay, J. Gulyás, J. Tímár, T. Kibédi, and V. Paar, Fizika **22**, 1 (1990).

[26] V. Paar, Nucl. Phys. **A331**, 16 (1979); Z. Árvay, T. Fényes, J. Gulyás, T. Kibédi, E. Koltay, A. Krasznahorkay, S. László, V. Paar, S. Brant, and Z. Hlousek, Z. Phys. A **299**, 139 (1981).

[27] P. Raghavan, At. Data Nucl. Data Tables **42**, 189 (1989).